



HAL
open science

Aligned High Density Semi-Conductive Ultra-Small Single-Walled Carbon Nanotubes

Yun Wang, Teng Ben, Shilun Qiu, Valentin Valtchev

► **To cite this version:**

Yun Wang, Teng Ben, Shilun Qiu, Valentin Valtchev. Aligned High Density Semi-Conductive Ultra-Small Single-Walled Carbon Nanotubes. *ChemistrySelect*, 2019, 4 (43), pp.12676-12679. 10.1002/slct.201904178 . hal-03033927

HAL Id: hal-03033927

<https://normandie-univ.hal.science/hal-03033927>

Submitted on 17 Dec 2020

HAL is a multi-disciplinary open access archive for the deposit and dissemination of scientific research documents, whether they are published or not. The documents may come from teaching and research institutions in France or abroad, or from public or private research centers.

L'archive ouverte pluridisciplinaire **HAL**, est destinée au dépôt et à la diffusion de documents scientifiques de niveau recherche, publiés ou non, émanant des établissements d'enseignement et de recherche français ou étrangers, des laboratoires publics ou privés.

Aligned High Density Semi-Conductive Ultra-Small Single-Walled Carbon Nanotubes

Yun Wang,^[a] Teng Ben,^{*[a, b]} Shilun Qiu,^[a, b] and Valentin Valtchev^[b, c]

Zeolite type material (AIPO-5, AFI-type) with rod-like morphology and mono-dimensional channel system running along the long crystal axis was vertically grown on a stainless-steel plate. The organic template used in the synthesis was carbonized to generate single-walled carbon nanotubes (SWCNTs). Thus, SWCNTs with a diameter of 0.4 nm, perfectly aligned and vertically oriented to the support surface with a density of 2.6×10^5 SWCNTs μm^{-2} , were obtained. The free end of AIPO-5 crystal was chemically etched in order to create contact surface and measure the conductivity of SWCNT@AIPO-5 film which was found to be $4.16 \times 10^{-1} \Omega^{-1} \text{cm}^{-1}$. This approach of aligned SWCNTs can be applied to different types of substrates, thus opening the road to practical uses of SWCNTs.

Single-walled carbon nanotubes (SWCNTs) are the most plausible alternative of silicon-based electronic devices due to their exceptional transconductance and current-carrying capacity.^[1] Aviram and Ratner first proposed individual molecules as functional electronic devices and opened the route to molecular electronics.^[2] The discovery of multi-walled carbon nanotubes (MWCNTs) by Iijima^[3] attracted the interest of different communities and the research in this field constantly grows.^[4–13] The next big step to nano/molecular electronics was the discovery of SWCNTs.^[14,15] However, the exceptional potential of SWCNTs can only be explored if they are properly integrated into electronic devices.^[16–19] Arrays of SWCNTs would be ideal for electronic devices if the tubes are aligned and tightly packed. Traditional preparation methods of SWCNTs include arc discharge,^[14] laser ablation^[20] and chemical vapour deposition (CVD).^[21] In the past decade the research efforts were dedicated to the preparation of arrays of densely packed SWCNTs in order to improve the current drive capability, transconductance and cut-off frequency in applied devices prototypes as electrochemical capacitors,^[22] and integrated circuits in digital and radio frequency electronics.^[23] Researchers from IBM pointed out that a density of 125 SWCNTs μm^{-1} will

have to be achieved in order for carbon nanotubes to be included in integrated circuits (IC).^[24] At present, the preparation of large-area high-density nanotube arrays is still a challenge, although various physical and chemical approaches have been employed.^[25–36] Misalignment and non-uniformity of carbon nanotube arrays are the major roadblocks to the practical uses. An alternative approach that could circumvent these difficulties is the use of a porous scaffold that controls the alignment and density of SWCNTs.^[37–39] Microporous zeolite type crystals with Angstrom size well define pore system present a perfect scaffold for such preparation.^[40] The strategy of this work was to select porous materials with ideal straight channels as templates, and AIPO_{4-n} family molecular sieves were preferred. As a one-dimensional quantum wires, carbon nanotubes have different conductivity due to their different sizes, the thinner in diameter and smaller the spacing between the tubes, the higher density arrangement of the same area would be. Moreover Tang et al. have already demonstrated the possibility to grow 0.4 nm SWCNTs in AIPO-5 (AFI-type) crystals.^[41] Here we report a method that allows fabricating ultra-high densely packed and aligned SWCNTs.

Film of densely packed AIPO-5 crystals was grown on a stainless-steel substrate with size 4 x 4 cm (Figure 1A, B). The

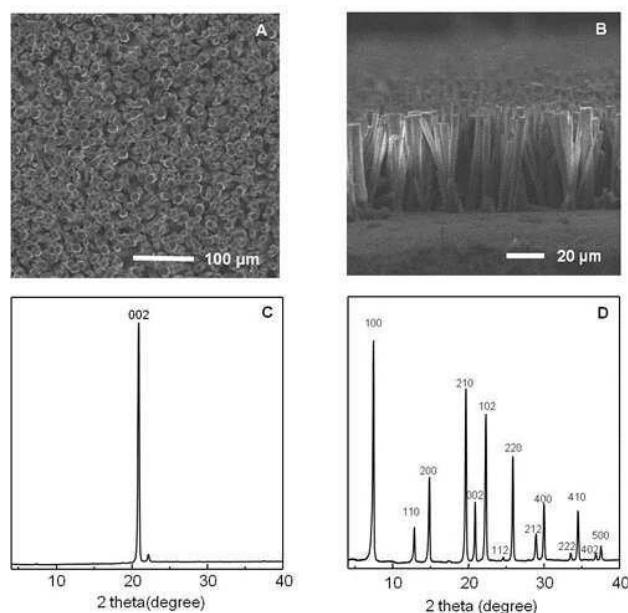


Figure 1. Top (A) and cross-section (B) SEM images of AIPO-5 film. Thin film (C) and powder (D) XRD patterns of AIPO-5.

[a] Y. Wang, Prof. T. Ben, Prof. S. Qiu
Zhuhai College of Jilin University, Zhuhai,
China E-mail: tben@jlu.edu.cn

[b] Prof. T. Ben, Prof. S. Qiu, Prof. V. Valtchev
Department of Chemistry, Jilin University, Changchun, China

[c] Prof. V. Valtchev
Normandie Univ, ENSICAEN, UNICAEN, CNRS, Laboratoire
Catalyse et Spectrochimie, 6 Marechal Juin, 14050 Caen, France

Supporting information for this article is available on the WWW under
<https://doi.org/10.1002/slct.201904178>

crystals building the film are 5 x 100 μm in size, exhibiting the typical of AIPO-5 hexagonal prism morphology. The long c-axis, along which is running the twelve-membered ring channel, is vertically oriented to the substrate surface. The vertical orientation of the crystals is confirmed by the XRD pattern of the film where the (002) peak is very intense. The height of (102) peak is reduced substantially (Figure 1C) and the intense peaks with (h00) or (hk0) indices are not visible (Figure 1D). The carbon nanotubes were formed by pyrolysis between 450 $^{\circ}\text{C}$ and 800 $^{\circ}\text{C}$ of the organic template used in the synthesis of AIPO-5. The process was optimized by using different organic templates and pyrolysis conditions.^[42,43] The sample obtained at 800 $^{\circ}\text{C}$ showed the best performance and was selected for more detailed analysis. Being pyrolyzed in vacuum at 800 $^{\circ}\text{C}$ the film remains intact as confirmed by the SEM analysis (Figure S2). The 0.4 nm SWCNTs prepared are aligned and stable when confined in the AFI framework. However, after extraction from the AFI channel system the self-standing nanotubes is difficult to be employed for practical uses due to the strong curvature effect.

No N H band (3174-3241 cm^{-1}) was observed in the IR spectrum of pyrolyzed sample revealing the full conversion of TrPA (tripropylamine) template (Figure S1). The impact of the temperature of pyrolysis on the formation of SWCNTs was studied by Raman spectroscopy (Figure 2, Table 1). The Raman spectrum of SWCNTs comprises three main segments.^[44] The

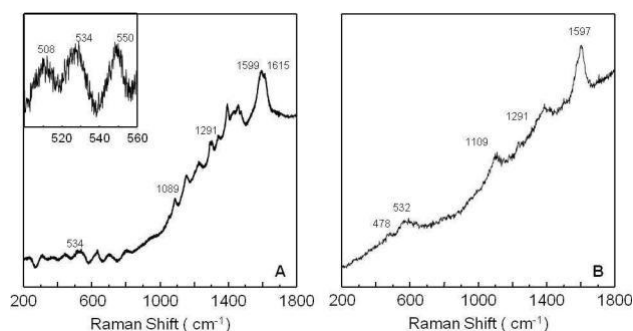


Figure 2. Raman spectra of SWCNTs@AIPO-5 film subjected to pyrolysis at 800 $^{\circ}\text{C}$: (A) before and (B) after etching.

Table 1. Raman bands of the SWCNTs@AIPO-5 thin films obtain after carbonization at different temperatures			
Carbonization temperature ($^{\circ}\text{C}$)	RBM frequencies (400-600 cm^{-1})	D band frequencies (1200-1500 cm^{-1})	G band frequencies (1500-1620 cm^{-1})
450	533	1237,1337,1441	1580
500	537	1224,1335,1452	1588
550	529	1219,1338,1441	1572
600	533	1241,1343,1451	1580
650	536	1249,1335,1452	1588
700	532	1229,1337,1462	1600
750	533	1229,1288,1304, 1344,1394,1430, 1453,1473	1595,1614
800	534	1233,1291,1387, 1424,1453,1473	1599,1615

high-frequency region 1500–1620 cm^{-1} with the G bands near 1600 cm^{-1} corresponds to the tangential band stretching vibrations. The G band further split into two parts, G^+ (1615 cm^{-1}) and G (1599 cm^{-1}), due to the curvature effect. The intermediate-frequency region (1200-1500 cm^{-1}), with D band near 1350 cm^{-1} , corresponds to the carbons with some defects, as the most common case is atomic vacancy defect. The low-frequency region (200-800 cm^{-1}) with a peak centered near 530 cm^{-1} is attributed to tubular vibrations along the radial direction, which is specific of SWCNTs bearing tubular structures.^[39,45–47]

Figure 2A represents the Raman spectrum of SWCNTs@AIPO-5 film prior to etching, where the radial breathing mode (RBM) of SWCNTs@AIPO-5 at 508 and 550 cm^{-1} is assigned to the semiconducting (4, 2) and (5, 0) SWCNTs.^[48] The relative ratio of the RBM to G-band, namely $I_{\text{RBM}}/I_{\text{G}}$ values range between 0.1 and 4 for different carbon nanotube.^[49,50] In this work, the intensity of RBM bands at 534 cm^{-1} and the line width of the G-band in 1599 cm^{-1} was 0.19, indicating TrPA was well carbonized into SWCNT inside the AIPO-5 channel. After etching, the RBM bands shifted to lower frequency due to the weakened interaction between the AIPO-5 framework and SWCNTs wall (Figure 2B). The diameter of the SWCNTs (d_t) was estimated to be 0.42 \pm 0.02 nm by empirical formulas $\omega_{\text{RBM}} = A/d_t$ (ω_{RBM} is the RBM peak frequency, $A = 223.75 \text{ cm}^{-1} \text{ nm}^{[51]}$), which matches with the TEM observation.

The connection of ultra small carbon nanotubes formed in the zeolite channel to the measuring device is probably the most challenging part of this study. We achieved this by controlled etching of the AIPO-5 crystal in 0.15 M KOH ethanol solution. The treatment was performed at room temperature in order to slow down the etching kinetics. The best result was obtained after 25 days of etching. Figure 3A represents the

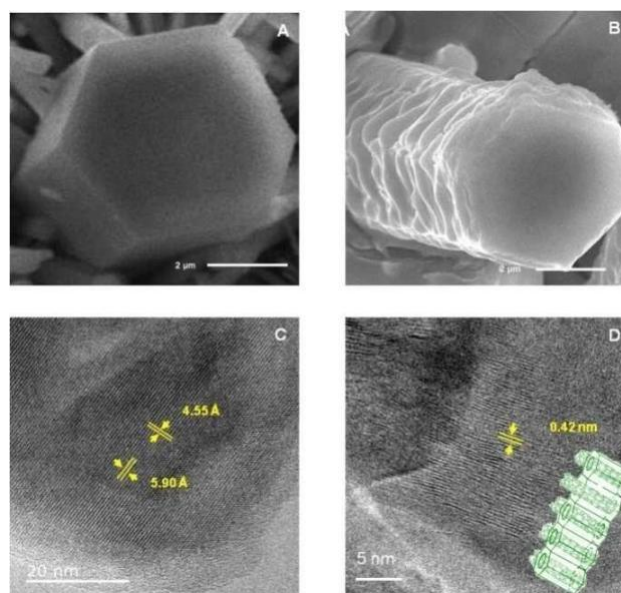


Figure 3. SEM images of AIPO-5 crystal prior to (A) and after etching (B) with 0.15 M KOH ethanol solution. High resolution TEM image of AIPO-5 crystal (C) and the free extremity of the carbon nanotubes after the crystal etching (D).

typical hexagonal prisms of AIPO-5 with straight and sharp edges on the pinacoidal face. After etching, the straight edges of AIPO-5 crystal (Figure 3A) became rounded and step of dissolution can be observed on the prismatic face (Figure 3B).

Figure 3C shows the [020] and [120] crystal plane of AIPO-5 crystal with interplanar space of 5.90 Å and 4.55 Å, respectively. Partly unmolded carbon nanotubes emerging from zeolite channels can be seen in Figure 3D. As revealed by the TEM study, the diameter of the SWCNTs obtained in the channels of AIPO-5 is 0.42 nm. It should be noted that SWCNT is unstable when all the AIPO-5 was removed by etching.^[37,52–54]

Thermogravimetric analysis (TGA) was used to estimate the SWCNTs content inside the AIPO-5 (Figure S3). Upon being heated to 600 °C in dry air, the SWCNTs@AIPO-5 film together with the substrate exhibits a weight loss of 0.8 wt.%. Thus, the formation yield of SWCNTs was evaluated to be 12.8%. Considered the size of the AIPO-5 crystals, the density of SWCNTs was estimated to be 2.6×10^5 SWCNTs μm^2 (or 162 SWCNTs μm^{-1}). To our best knowledge, this value is among the highest density of SWCNTs to date and surpasses the target (125 CNTs μm^{-1}) of IC.^[24] The electric transport properties of SWCNTs-containing film were studied after pasting double-sided carbon conductive tape, as shown in Figure 4A.

Current-voltage (I-V) properties are measured in the temperature of 27 °C (Figure 4B). The conductivity of the SWCNTs@AIPO-5 film is $1.31 \times 10^6 \Omega^{-1} \text{cm}^{-1}$. Given that each SWCNT in the film is connected in parallel, the conductivity of the single SWCNT inside the AIPO-5 channel is calculated to be $4.16 \times 10^1 \Omega^{-1} \text{cm}^{-1}$, which is comparable to the previous literature data.^[37]

The density of carbon nanotube reported previously is summarized in Figure 4C.^[55–62] As can be seen, our strategy provides SWCNTs with a higher density than previously reported methods with the exception of the horizontally

oriented CNTs prepared by Cao et al. using the Langmuir-Blodgett method.⁶³ However, the vertically aligned arrays show higher thermal conductivity and offer advantages for practical applications.^[64–67] Thus the present study represents a big step ahead not only the preparation of aligned densely packed SWCNTs, but also in their production in a form appropriate for practical uses. This work represents a robust method to achieve ultrahigh density vertically aligned SWCNTs arrays. Owing to the ultra-small diameter of the SWCNTs, which is much smaller than that of the silicon transistors (90 nm) currently used, the future integration density could be improved substantially. Consequently, the resistance loss of the wire and the capacitance between the wires will be reduced, accompanied by the increasing operating frequency and decreasing the energy consumption.^[59,68] This may well solve the signal delay problem in the application of logic circuits.

To summarize, AIPO-5 film-derived ultra-small vertically-oriented SWCNTs with diameter 0.4 nm were synthesized by pyrolysis of the organic (TrPA) template. The free-standing end of AIPO-5 crystals was etched in order to connect the ultra-small nano-tubes to a circuit. The conductivity of the SWCNTs@AIPO-5 film is $1.31 \times 10^6 \Omega^{-1} \text{cm}^{-1}$. The SWCNTs density is estimated to be 2.6×10^5 SWCNTs μm^2 (162 SWCNTs μm^{-1}) surpassing the target of 125 SWCNTs μm^{-1} postulated by Franklin.^[24] Each SWCNT in the film is connected in parallel. According to this fact, the conductivity of the single SWCNT@AIPO-5 was estimated to be $4.16 \times 10^1 \Omega^{-1} \text{cm}^{-1}$. The SWCNTs array is semiconductor type, and its size is far smaller than the dimensions of semiconductor materials currently used in computing and data storage. This material is expected to overcome the size limitation of silicon-based materials and have the potential to be used in electronic devices, significantly increasing computing speed and storage capacity.

Supporting Information Summary

The supporting information contains experimental procedures (Part 1), characterization and calculation process of materials (Part 2). References related to experimental section were show in Part 3 of supporting information. S1-S3 display the IR, XRD and TGA, the corresponding group attribution are also given.

Keywords: aligned SWCNTs · AIPO-5 · molecular wire · high density carbon nanotube

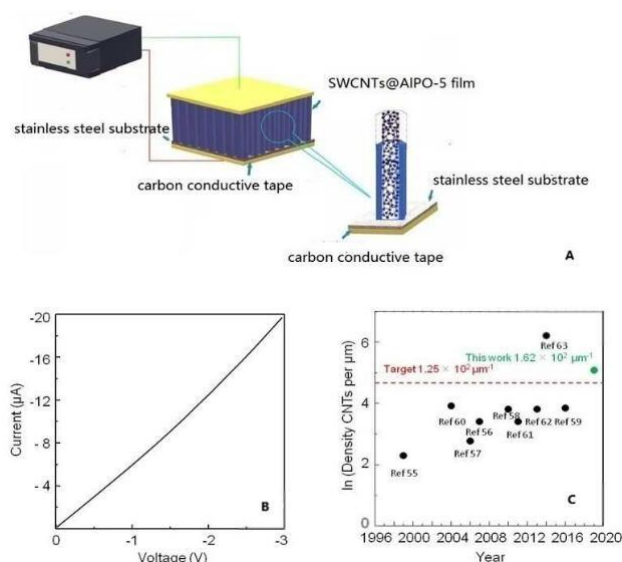


Figure 4. Schematic presentation of the experimental setup (A); I-V curve of SWCNTs@AIPO-5 film (B); and density of CNTs reported in the previous publications (C).

- [1] L. M. Peng, Z. Y. Zhang, S. Wang, *Mater. Today*, **2014**, *17*, 433–442.
- [2] A. Aviram, M. A. Ratner, *Chem. Phys. Lett.* **1974**, *29*, 277–283.
- [3] S. Iijima, *Nature*, **1991**, *354*, 56–58.
- [4] R. H. Baughman, A. A. Zakhidov, W. A. de Heer, *Science*, **2002**, *297*, 787–792.
- [5] K. Tanaka, S. Iijima, *Carbon Nanotubes and Graphene Edition 2*, Amsterdam: Elsevier publications, **2014**, pp. 155–200.
- [6] L. C. Qin, X. L. Zhao, K. Hirahara, Y. Miyamoto, Y. Ando, S. Iijima, *Nature*, **2000**, *408*, 50–50.
- [7] P. M. Ajayan, S. Iijima, *Nature*, **1992**, *358*, 23–23.
- [8] M. S. Dresselhaus, G. Dresselhaus, R. Saito, *Solid State Commun.* **1992**, *84*, 201–205.
- [9] L. F. Sun, S. S. Xie, W. Liu, W. Y. Zhou, Z. Q. Liu, D. S. Tang, G. Wang, L. X. Qian, *Nature*, **2000**, *403*, 384–384.

- [10] X. Zhao, M. Ohkohchi, M. Wang, S. Iijima, T. Ichihashi, Y. Ando, *Carbon*, **1997**, *35*, 775–781.
- [11] D. Ugarte, A. Châtelain, W. A. de Heer, *Science*, **1996**, *274*, 1897–1899.
- [12] D. L. Andrews, G. D. Scholes, G. P. Wiederrecht, *Comprehensive Nano-science and Technology*, Amsterdam: Elsevier publications, **2011**, pp. 23–39.
- [13] E. T. Thostenson, Z. Ren, T. W. Chou, *Compos. Sci. Technol.* **2001**, *61*, 1899–1912.
- [14] S. Iijima, T. Ichihashi, *Nature*, **1993**, *363*, 603–605.
- [15] D. S. Bethune, C. H. Kiang, M. S. de Vries, G. Gorman, R. Savoy, J. Vazquez, R. Beyers, *Nature*, **1993**, *363*, 605–607.
- [16] C. Joachim, J. K. Gimzewski, A. Aviram, *Nature*, **2000**, *408*, 541–548.
- [17] M. Bockrath, D. H. Cobden, P. L. McEuen, N. G. Chopra, A. Zettl, A. Thess, R. E. Smalley, *Science*, **1997**, *275*, 1922–1925.
- [18] S. J. Tans, M. H. Devoret, H. Dai, A. Thess, R. E. Smalley, L. J. Geerligs, C. Dekker, *Nature*, **1997**, *386*, 474–477.
- [19] S. J. Tans, A. R. M. Verschueren, C. Dekker, *Nature*, **1998**, *393*, 49–51.
- [20] A. Thess, R. Lee, P. Nikolaev, H. Dai, P. Petit, J. Robert, C. H. Xu, Y. H. Lee, S. G. Kim, A. G. Rinzler, D. T. Colbert, G. E. Scuseria, D. Tománek, J. E. Fischer, R. E. Smalley, *Science*, **1998**, *273*, 483–487.
- [21] H. J. Dai, A. G. Rinzler, P. Nikolaev, A. Thess, D. T. Colbert, R. E. Smalley, *Chem. Phys. Lett.* **1996**, *260*, 471–475.
- [22] K. H. An, W. S. Kim, Y. S. Park, *Adv. Mater.* **2006**, *13*, 497–500.
- [23] Y. C. Che, H. T. Chen, H. Gui, J. Liu, B. L. Liu, C. W. Zhou, *Semicond. Sci. Technol.* **2014**, *29*, 073001
- [24] A. D. Franklin, *Nature*, **2013**, *498*, 443–444.
- [25] Y. Hu, L. X. Kang, Q. C. Zhao, H. Zhong, S. C. Zhang, L. W. Yang, Z. Q. Wang, J. J. Lin, Q. W. Li, Z. Y. Zhang, L. M. Peng, Z. F. Liu, J. Zhang, *Nat. Commun.* **2015**, *6*, Article ID 6099.
- [26] X. F. Duan, Y. Huang, Y. Cui, J. F. Wang, C. M. Lieber, *Nature*, **2001**, *409*, 66–69.
- [27] A. Ural, Y. M. Li, H. J. Dai, *Appl. Phys. Lett.* **2002**, *81*, 3464–3466.
- [28] S. M. Huang, B. Maynor, X. Y. Cai, J. Liu, *Adv. Mater.* **2003**, *15*, 1651–1655.
- [29] W. W. Zhou, Z. Y. Han, J. Y. Wang, Y. Zhang, Z. Jin, X. Sun, Y. W. Zhang, C. H. Yan, Y. Li, *J. Am. Chem. Soc.* **2006**, *6*, 2987–2990.
- [30] Y. Huang, X. F. Duan, Q. Q. Wei, C. M. Lieber, *Science*, **2001**, *291*, 630–633.
- [31] N. A. Melosh, A. Boukai, F. Diana, B. Gerardot, A. Badolato, P. M. Petroff, J. R. Heath, *Science*, **2003**, *300*, 112–115.
- [32] W. A. Lopes, H. M. Jaeger, *Nature*, **2001**, *414*, 735–738.
- [33] S. G. Rao, L. Huang, W. Setyawan, S. H. Hong, *Nature*, **2003**, *425*, 36–37.
- [34] H. Yan, S. H. Park, G. Finkelstein, J. H. Reif, T. H. LaBean, *Science*, **2003**, *301*, 1882–1884.
- [35] A. Ismach, L. Segev, E. Wachtel, E. Joselevich, *Angew. Chem., Int. Ed.* **2004**, *116*, 6266–6269.
- [36] C. Kocabas, S. H. Hur, A. Gaur, M. A. Meitl, M. Shim, J. A. Rogers, *Small*, **2005**, *1*, 1110–1116.
- [37] Z. K. Tang, H. D. Sun, J. Wang, J. Chen, G. Li, *Appl. Phys. Lett.* **1998**, *73*, 2287–2289.
- [38] Z. K. Tang, N. Wang, X. X. Zhang, J. N. Wang, C. T. Chan, P. Sheng, *New J. Phys.* **2003**, *5*, 146.1-146.29.
- [39] M. Hulman, H. Kuzmany, O. Dubay, G. Kresse, L. Li, Z. K. Tang, *J. Chem. Phys.* **2003**, *119*, 3384–3390.
- [40] <http://www.iza-structure.org/databases/>
- N. Wang, Z. K. Tang, G. D. Li, J. S. Chen, *Nature*, **2000**, *408*, 50–51.
- [41] J. P. Zhai, Z. K. Tang, F. L. Y. Lam, X. J. Hu, *J. Phys. Chem. B.* **2006**, *110*, 19285–19290.
- [42] H. D. Sun, Z. K. Tang, J. Chen, G. Li, *Solid State Commun.* **1999**, *109*, 365–369.
- [43] N. Saifuddin, A. Z. Raziah, A. R. Junizah, *J. Chem.* **2012**, *2013*, Article ID 676815.
- [44] S. Reich, C. Thomsen, J. Maultzsch, *Carbon nanotubes: basic concepts and physical properties*, Wiley-VCH Verlag GmbH & Co. KGaA, **2004**, 115–133.
- [45] M. S. Dresselhaus, G. Dresselhaus, A. Jorio, A. G. Souza Filho, R. Saito, *Carbon*, **2002**, *40*, 2043–2061.
- [46] R. Saito, G. Dresselhaus, M. S. Dresselhaus, *Physical Properties of Carbon Nanotubes*, Amsterdam: Imperial College Press, **1998**, pp. 183–203.
- [47] O. Dubay, G. Kresse, *Phys. Rev. B*, **2003**, *67*, Article ID 035401.
- [48] G. S. Duesberg, I. Loa, M. Burghard, K. Syassen, S. Roth, *Phys. Rev. Lett.* **2000**, *85*, 5436–5439.
- [49] J. P. Zhai, Z. K. Tang, X. J. Hu, X. X. Zhang, P. Sheng, *Phys. Status Solidi (B)*, **2006**, *243*, 3082–3086.
- [50] S. Bandow, S. Asaka, Y. Saito, A. M. Rao, L. Grigorian, E. Richter, P. C. Eklund, *Phys. Rev. Lett.* **1998**, *80*, 3779–3282.
- [51] L. M. Peng, Z. L. Zhang, Z. Q. Xue, Q. D. Wu, Z. N. Gu, D. G. Pettifor, *Phys. Rev. Lett.* **2000**, *85*, 3249–3252.
- [52] D. H. Robertson, D. W. Brenner, J. W. Mintmire, *Phys. Rev. B*, **1992**, *45*, 12592–12595.
- [53] J. Tersoff, *Phys. Rev. Lett.* **1988**, *61*, 2879–2882.
- [54] J. Li, C. Papadopoulos, J. M. Xu, M. Moskovits, *Appl. Phys. Lett.* **1999**, *75*, 367–369.
- [55] X. L. Li, L. Zhang, X. R. Wang, I. Shimoyama, X. M. Sun, W. S. Seo, H. J. Dai, *J. Am. Chem. Soc.* **2007**, *129*, 4890–4891.
- [56] Y. M. Choi, S. Lee, H. S. Yoon, M. S. Lee, H. J. Kim, I. Han, Y. Son, I. Yeo, U. Chung, J. T. Moon, **2006**, Sixth IEEE Conference on Nanotechnology
- [57] A. D. Franklin, A. Lin, H. S. P. Wong, Z. H. Chen, *IEEE Electr. Device L.* **2010**, *31*, 644–646.
- [58] G. J. Brady, A. J. Way, N. S. Safron, H. T. Evensen, P. Gopalan, M. S. Arnold, *Sci. Adv.* **2016**, *2*, Article ID e1601240
- [59] W. Hoenlein, F. Kreupl, G. S. Duesberg, A. P. Granham, M. Liebau, R. V. Seidel, E. Unger, *IEEE T. Comp. Pack. Man.* **2004**, *27*, 629–634.
- [60] H. Ago, T. Ayagaki, Y. Ogawa, M. Tsuji, *J. Phys. Chem. C*, **2011**, *115*, 13247–13253.
- [61] Y. Chen, J. Zhang, *Accounts Chem. Res.* **2014**, *47*, 2273–2281.
- [62] Q. Cao, S. J. Han, G. S. Tulevski, Y. Zhu, D. D. Lu, W. Haensch, *Nat. Nanotechnol.* **2013**, *8*, 180–186.
- [63] S. Berber, Y. K. Kwon, D. Tomanek, *Phys. Rev. Lett.* **2000**, *84*, 4613–4616.
- [64] A. V. Savin, B. Hu, Y. S. Kivshar, *Phys. Rev. B*, **2009**, *80*, Article ID 15423.
- [65] W. Choi, S. Hong, J. T. Abrahamson, J. H. Han, C. Song, N. Nair, S. Baik, M. S. Strano, *Nat. Mater.* **2010**, *9*, 423–429.
- [66] R. F. Zhang, Y. Y. Zhang, F. Wei, *Chem. Soc. Rev.* **2017**, *46*, 3661–3715.
- [67] C. Rutherglen, D. Jain, P. Burke, *Nat. Nanotechnol.* **2009**, *355*, 811–819.

Submitted: November 1, 2019

Accepted: November 7, 2019